


## ARTICLE



# Deep phenotypic characterization of the retinal dystrophy in patients with *RNU4ATAC*-associated Roifman syndrome

Brian G. Ballios<sup>1</sup>, Amarilla Mandola<sup>2</sup>, Alaa Tayyib<sup>1,3</sup>, Anupreet Tumber<sup>3</sup>, Jenny Garkaby<sup>2</sup>, Linda Vong<sup>4</sup>, Elise Heon<sup>1,3</sup>, Chaim M. Roifman<sup>2,4</sup> and Ajoy Vincent<sup>1,3</sup> 

© Crown 2023

**PURPOSE:** To characterize the retinal phenotype in *RNU4ATAC*-associated Roifman syndrome.

**METHODS:** Ten patients (including 8 males) with molecularly confirmed Roifman syndrome underwent detailed ophthalmologic evaluation including fundus imaging, fundus autofluorescence (FAF) imaging, spectral-domain optical coherence tomography (SD-OCT), and electroretinography (ERG). Six patients had follow-up eye exams. All patients also underwent comprehensive examination for features of extra-retinal Roifman syndrome.

**RESULTS:** All patients had biallelic *RNU4ATAC* variants. Nyctalopia was common (7/10). Visual acuity at presentation ranged from 20/20 to 20/200 (Age Range: 5–41 years). Retinal exam revealed features of generalized retinopathy with mid-peripheral pigment epithelial changes. A para or peri-foveal ring of hyper-autofluorescence was the commonest FAF abnormality noted (6/8). The SD-OCT demonstrated relative preservation of the foveal ellipsoid zone in six cases; associated features included cystoid changes (5/10) and posterior staphyloma (3/10). The ERG was abnormal in all patients; nine showed generalized rod-cone dystrophy, whilst one patient with sectoral retinal involvement only had isolated rod dystrophy (20 years old). On follow-up examination (Mean duration: 8.16 years), progressive loss of visual acuity (2/6), mid-peripheral retinal atrophy (3/6) or shortening of ellipsoid zone width (1/6) were observed.

**CONCLUSION:** This study has characterized the retinal phenotype in *RNU4ATAC*-associated Roifman syndrome. Retinal involvement is universal, early-onset, and overall, the retinal and FAF features are consistent with rod-cone degeneration that is slowly progressive over time. The sub-foveal retinal ultrastructure is relatively preserved in majority of patients. Phenotypic variability independent of age exists, and more study of allelic- and sex-based determinants of disease severity are necessary.

Eye (2023) 37:3734–3742; <https://doi.org/10.1038/s41433-023-02581-1>

## INTRODUCTION

Roifman syndrome is an autosomal recessive disorder originally described as a novel association of immunodeficiency, spondyloepiphyseal dysplasia, developmental delay, facial dysmorphism, and retinal dystrophy [1], caused by biallelic variants in the small nuclear RNA (snRNA) *U4atac* (*RNU4ATAC*) [2, 3]. The *U4atac* snRNA, is a component of the minor spliceosome that regulates the correct splicing of around 800 genes [2]. At least one *RNU4ATAC* variant must obligatorily involve its Stem II region to cause Roifman syndrome [3]. Homozygous or compound heterozygous variants in *RNU4ATAC* have also been associated with microcephalic osteodysplastic primordial dwarfism type 1 (MOPD1) [4, 5].

To date, 18 patients affected with Roifman syndrome have been described in the literature [1–3, 6–14]. Retinal involvement has been reported in the syndrome, observed in nine cases [1–3, 11, 12]. The retinal description includes hypo-vascularization and attenuated retinal vessels [2, 3, 12], retinal pigment epithelial (RPE) changes [3, 11], variable optic disc pallor [3, 12], and occasional reports of dull

foveal reflex [3] or macular oedema [12]. Variable degree of generalized retinal dysfunction has been reported using full-field electroretinography (ERG) in three cases [1, 11]. There is a single case report that describes fundus autofluorescence (FAF) findings [11], whilst none describe optical coherence tomography (OCT) features, and overall, the retinal phenotype associated with Roifman syndrome has not been comprehensively characterized.

The current study characterizes in detail the ophthalmological phenotype in a cohort of ten patients with molecularly confirmed *RNU4ATAC*-related Roifman syndrome. With this large case series, we describe the natural history and characteristic retinal changes spanning four decades of disease. This series includes the youngest reported case with retinal involvement (a 6-month-old infant) as well as a young adult with sectoral-retinal disease.

## METHODS

The study protocol adhered to the tenets of the Declaration of Helsinki and was approved by the research ethics board at the Hospital for Sick

<sup>1</sup>Department of Ophthalmology and Vision Sciences, University of Toronto, Toronto, ON, Canada. <sup>2</sup>Division of Immunology and Allergy, The Hospital for Sick Children and the University of Toronto, Toronto, ON, Canada. <sup>3</sup>Department of Ophthalmology and Vision Sciences, The Hospital for Sick Children, Toronto, ON, Canada. <sup>4</sup>The Canadian Centre for Primary Immunodeficiency and The Jeffrey Modell Research Laboratory for the Diagnosis of Primary Immunodeficiency, The Hospital for Sick Children, Toronto, ON, Canada.

<sup>✉</sup>email: [ajoy.vincent@sickkids.ca](mailto:ajoy.vincent@sickkids.ca)

Received: 30 December 2022 Revised: 1 May 2023 Accepted: 11 May 2023

Published online: 24 May 2023

Children, Toronto, Canada. Patient information was collected prospectively and retrospectively from medical records and entered to the Canadian Centre for Primary Immunodeficiency Registry. Informed consent was obtained from all patients.

### Ophthalmic assessment

Ten patients (cases 9 and 10 are siblings) with biallelic variants in *RNU4ATAC* and confirmed Roifman syndrome phenotype were recruited. The genetic variants and clinical features (mostly systemic features with limited retinal phenotypic information) of 5 cases have been previously reported [Cases 7, 9 and 10 [2] and Cases 2 and 4 [3], respectively]. A comprehensive history and detailed eye examination was performed that included: best-corrected visual acuity (BCVA) and color vision assessment (Hardy-Rand-Rittler plates), contrast sensitivity measurement [15] and retinal evaluation. The eye with better acuity was used to summarize the data. Fundus photographs were obtained in all subjects whereas, FAF imaging was performed on eight patients. Spectral-domain OCT (SD-OCT) imaging (Cirrus, Carl Zeiss Meditec or Spectralis, Heidelberg Engineering or Envisu C2300, Bioptigen) included acquisition of horizontal raster scans centred at the fovea (at least 6 mm length; all patients) and volume scans (macular cube 6 × 6 mm – 128 horizontal scan lines comprising 1024 A-scans each; 7 patients). Central sub-foveal thickness (CST) and average macular cube thickness were measured, when possible. Full-field ERG testing based on International Society for Clinical Electrophysiology of Vision Standard stimuli [16] was performed in all cases. The ERG testing was performed under chloral hydrate sedation (Case 1), general anesthesia (Case 2) or awake ( $n = 8$ ), using corneal Jet™ (Cases 1 and 2), Dawson-Trick-Litzkow (DTL; 7 cases) or Ambu® Neuroline™ 700 skin electrodes (Case 5). Pattern ERG was done in 9 patients using DTL electrodes [17]. Although visual field testing was attempted, significant developmental delay precluded reliability and hence, these results were not included in this study.

Pearson's correlations were performed to evaluate the relationship between age and BCVA (average visual acuity of the two eyes), and between age and the following ERG parameters: I. Dark adapted (DA) 0.01 b-wave amplitude, II. DA 10 a-wave amplitude, III. DA 10 a-wave implicit time, IV. DA 10 ERG b-wave amplitude, V. DA 10 ERG b-wave implicit time, VI. Light adapted (LA) 3.0 2 Hz a-wave amplitude, VII. LA 3.0 2 Hz a-wave implicit time, VIII. LA 3.0 2 Hz b-wave amplitude, IX. LA 3.0 2 Hz b-wave implicit time, X. LA 30 Hz flicker amplitude and XI. LA 30 Hz flicker implicit time. Linear regressions were also performed to assess whether age predicted average visual acuity, and whether age predicted the ERG parameters.

### Systemic evaluation

Each patient underwent comprehensive workup by the immunodeficiency service, including a focused history and clinical characteristics, including presence of growth deficiency (e.g., intrauterine growth restriction); neurologic manifestations (e.g., developmental delay); skeletal anomalies (e.g., spondyloepiphyseal dysplasia); cardiac manifestations; endocrine dysfunction; renal disease; and immune abnormalities. Serum immunoglobulin profile, viral, and post-vaccine titre immune workup was also performed.

### Genetic analysis

Patient's genomic DNA was extracted from lymphocytes [3], and PCR amplified using specific primers designed for the *RNU4ATAC* gene (details available on request). Sequencing was done using GenomeLab Dye Terminator Cycle Sequencing Quick Start Kit (Beckman Coulter) and analyzed on CEQ 8000 Genetic Analysis System (Beckman Coulter).

## RESULTS

Eight males and two females participated in the study. Age at first visit ranged from 6 months to 41 years. Six patients had more than one eye exam; the follow-up period ranged from 2 to 19 years (Median: 4.5 years; Mean: 8.16 years). Details of the eye phenotype of all ten affected individuals are summarized in Table 1 and supplementary Table 1.

Nyctalopia, though not always noticed at presentation, was observed in 7 cases; its onset ranged from 2 to almost 20 years of age. Hemeralopia was noted in 2 cases in late teens and early adulthood, respectively. None of the patients had nystagmus.

At presentation, the BCVA (Range: 5–41 years of age; Case 1 excluded) ranged from 20/20 to 20/200 (Median: 20/40); three had a BCVA better than 20/25 in either eye (Cases 3, 6, 7) (Table 1). Amongst patients who had multiple visits, two showed a two-line decline in Snellen acuity in at least 1 eye (Cases 2 and 7 over 3 and 17 years, respectively). However, there was no significant correlation between age and average visual acuity,  $r(8) = -0.0023$ ,  $p = 0.99$ . Moreover, age was not a significant predictor of visual acuity ( $F(1, 14) = 0.000071$ ,  $p = 0.99$ ;  $\beta = -0.0001$ ,  $p = 0.99$ ). Hypermetropia was seen in the majority ( $n = 7$ ) with or without astigmatism. Color vision was variably affected (Table 1) but contrast sensitivity was reduced in the majority (5/7).

The characteristics of the retinal phenotype appear in Figs. 1 and 2, Supplementary Fig. 1 and are summarized in Supplementary Table 1. The fundus appearance was generally characterized (except Cases 1 and 6, discussed separately) by diffuse yet discrete mid-peripheral hypo-pigmented dots at the level of RPE with mild pigmentary disturbances and attenuated arterioles. Discrete scalloped patches of chorioretinal atrophy were seen in two of the older cases (Ages, 33 and 41 years). Granular, discrete and deep hyperpigmented spots were seen in the mid-periphery in Cases 8 and 9 (Supplementary Fig. 1). A dull foveal reflex was observed in 7 cases.

Fundus autofluorescence was available in 8 cases; six of them had a para-/peri foveal ring of hyper-autofluorescence (Figs. 1 and 2). The diameter of the ring appeared broadest in Case 2 (at 5 and 8 years, respectively) compared to others ( $\geq 10$  years; Cases 3, 4, Cases 7–9). In cases 7 and 8 (aged 26 years), the ring appeared very close to the foveal centre. A mid-peripheral hypo-autofluorescence corresponding to the RPE changes was noted in 7 cases (except Case 6), and the extent of hypo-autofluorescence tended to increase in older individuals. The extent of mid-peripheral hypo-autofluorescence increased with increasing age in Cases 2 and 3 (Fig. 1). Case 10 had sub-optimal AF images, regardless, they demonstrated hyper-autofluorescence in the posterior pole with mid-peripheral hypo-autofluorescence. Further, the oldest patients (siblings; Cases 9 and 10) demonstrated mid-peripheral nummular hypo-autofluorescence patches, that corresponded to RPE atrophy seen on widefield imaging.

The SD-OCT showed outer retinal lamination to be variably affected (Figs. 1, 2 and Supplementary Table 1). Horizontal line scan through the fovea showed preservation of ellipsoid zone (EZ) in the central 2 mm in 6 patients (Cases 2, 3, 6, 7, 9, 10), whilst others demonstrated mild (Cases 4, 5, 8) or significant (Case 1) disruption. Case 5 that had 10-year follow-up scans showed progressive loss of EZ and external limiting membrane (ELM) (Fig. 2C, F). In the temporal macula, the EZ was attenuated or lost in all patients except Cases 6 and 10. The external limiting membrane (ELM) could be identified beyond the boundaries of EZ loss in all cases. Cystoid/schitic macular changes were present in 5 patients, and ranged from mild (Cases 3, 5, 8; Age Range: 10–26 years), to moderate (Case 4; 13 years), or severe (Case 1; infancy and at 2 years). The CST ranged between 211 and 330  $\mu\text{m}$  (RE;  $n = 7$ ; mean = 267.7  $\mu\text{m}$ ; median = 258  $\mu\text{m}$ ); three had cystoid changes. The average macular thickness ranged between 192 and 312  $\mu\text{m}$  (RE;  $n = 5$ ; mean = 251.2  $\mu\text{m}$ ; median = 253  $\mu\text{m}$ ); cases 4 and 7 had reduced average macular thickness (192 and 240  $\mu\text{m}$ , respectively).

The ERG traces are presented in Supplementary Figs. 2 and 3 and summarized in Supplementary Table 1. Nine patients showed a generalized rod-cone dystrophy, of which three had non-detectable rod and cone responses (Cases 4, 6 and 10 at 15, 19 and 40 years, respectively). Case 6 had isolated involvement of the rod system. Age was not significantly correlated to any ERG parameter ( $r(8) < \pm 0.51$ ,  $p > 0.10$ ). Furthermore, age was not a significant predictor of any ERG parameter ( $p > 0.10$ ). The pattern ERG showed reduced P50 amplitude consistent with macular dysfunction in 8 patients; Case 6 had normal pattern ERG.

**Table 1.** Eye phenotype at presentation and most recent follow up, systemic features and genetic results.

Case/Sex	Nucleotide Alteration	Age, y	Salient History, Symptoms, Signs	BCVA (OD: OS); Refraction (OD: OS)	Color Vision	CS (OD: OS)	Syndromic Features <sup>a</sup>
1/M	n.17 G > A / n.116 A > G	6 mo. 2	Makes eye contact Nyctalopia	1.3 cpd; 1.3 cpd 0.2 logMAR; 0.2 logMAR; +2.00; +2.00	NR NR	NR NR	Spondylo-epi-methaphyseal dysplasia; IUGR; micromelia; brachydactyly; clinodactyly
2/F	n.16 G > A / n.16 G > A <sup>d</sup>	5	No nyctalopia or hemeralopia; RXT 40 PD, Right IOOA	20/60; 20/50; -0.50/+1.50 x 090; +1.00/+3.00 x 180	NA	NA	DD; bilateral clindodactyly of fifth finger; spondyloepiphyseal dysplasia; IUGR; FTT; dysmorphism; mild conductive hearing loss
3/M	n.13 C > T / n.48 G > A	8 10 13	Nyctalopia, s/p Right MR resection/ Right LR recession; OD suppression No nyctalopia or hemeralopia; orthophoric Nyctalopia	20/125; 20/50; Plano; +0.50 x 180 20/25; 20/25; +1.50ds; +1.50ds 20/32; 20/32; +1.50; +1.50	Normal OU NA	1.2; 1.2 NA	DD; FTT; skeletal epiphyseal dysplasia; conductive and sensorineural hearing loss; dysmorphism; hypo-gonadotrophic hypogonadism
4/M	n.17 G > A / n.116 A > G <sup>d</sup>	7	Nyctalopia	20/100; 20/150; -1.00/+4.50 x 100; -0.50/+4.00 x 080	Normal	NA	DD; spondyloepiphyseal dysplasia; IUGR; dysmorphism
5/M	n.13 C > G / n.29 T > C <sup>e</sup>	13 6 25	Nyctalopia, Orthophoric No nyctalopia or hemeralopia. Right XT 30PD, patched OS. Nyctalopia and hemeralopia. Selective mutism.	20/80; 20/80; -0.50/+2.50 x 100; -0.25/+3.00 x 095 0.2 logMAR; 0.2 logMAR 20/100; 20/80; +1.00/+1.00 x 090; +1.00/+1.00 x 090	Mild BY deficit OU	1.1; 1.1 NA NR	DD; ichtthyosis vulgaris; IUGR; dysmorphism
6/F	n.13 C > T / n.46 G > A	20	Hemeralopia since late teens; no nyctalopia, no color vision concerns	20/20; 20/25; -2.00/+1.50 x 100; -2.00/+1.25 x 093	NA	1.7; 1.6	DD; learning difficulties; IUGR; FTT; scoliosis; rudimentary bilateral 12th ribs; dysmorphism
7/M	n.13 C > T / n.48 G > A <sup>c</sup>	10 26	Nyctalopia; constricted field; orthophoric Nyctalopia; constricted field	20/20; 20/20; +2.50; +2.00 20/32; 20/40; +5.50; +3.25 (at 17 Y)	NA Mild RG deficit OU	NA 1.7; 1.6	DD; poor weight gain; skeletal epiphyseal dysplasia; IUGR; dysmorphism
8/M	n.16 G > A / n.50 G > A / n.55 G > A	26	No nyctalopia or hemeralopia; Left/AXT, s/p strabismus surgery.	20/200; 20/300; +1.00; +2.00	NR	NA	DD; IUGR; FTT; skeletal dysplasia; dysmorphism
9/M <sup>b</sup>	n.13 C > T / n.37 G > A <sup>c</sup>	33	No nyctalopia or hemeralopia	20/80; 20/40; +1.50; +1.50; +1.00 x 090	NA	1.2; 1.2	DD; spondyloepiphyseal dysplasia; IUGR; dysmorphism
10/M <sup>b</sup>	n.13 C > T / n.37 G > A <sup>c</sup>	41	Nyctalopia for 20 years; loss of peripheral vision; cataract surgery OD, dense PSC OS.	20/40; 20/63; Refraction NA	Normal	1.4; 0.7	DD; epiphyseal dysplasia; dysmorphism

OD right eye, OS left eye, OU both eyes, BCVA best-corrected visual acuity, CS contrast sensitivity, PD prism diopters, VF visual field, NA not available, NR nonrecordable, UR unreliable, XT exotropia, AXT alternating exotropia, IOOA inferior oblique overaction, MR medial rectus, LR lateral rectus, s/p status-post, PSC posterior subcapsular cataract, IUGR intrauterine growth restriction, FTT failure to thrive, DD developmental delay.

<sup>a</sup>Gammaglobulin deficiency and infection (sino-pulmonary and otitis media) details are included in main text.

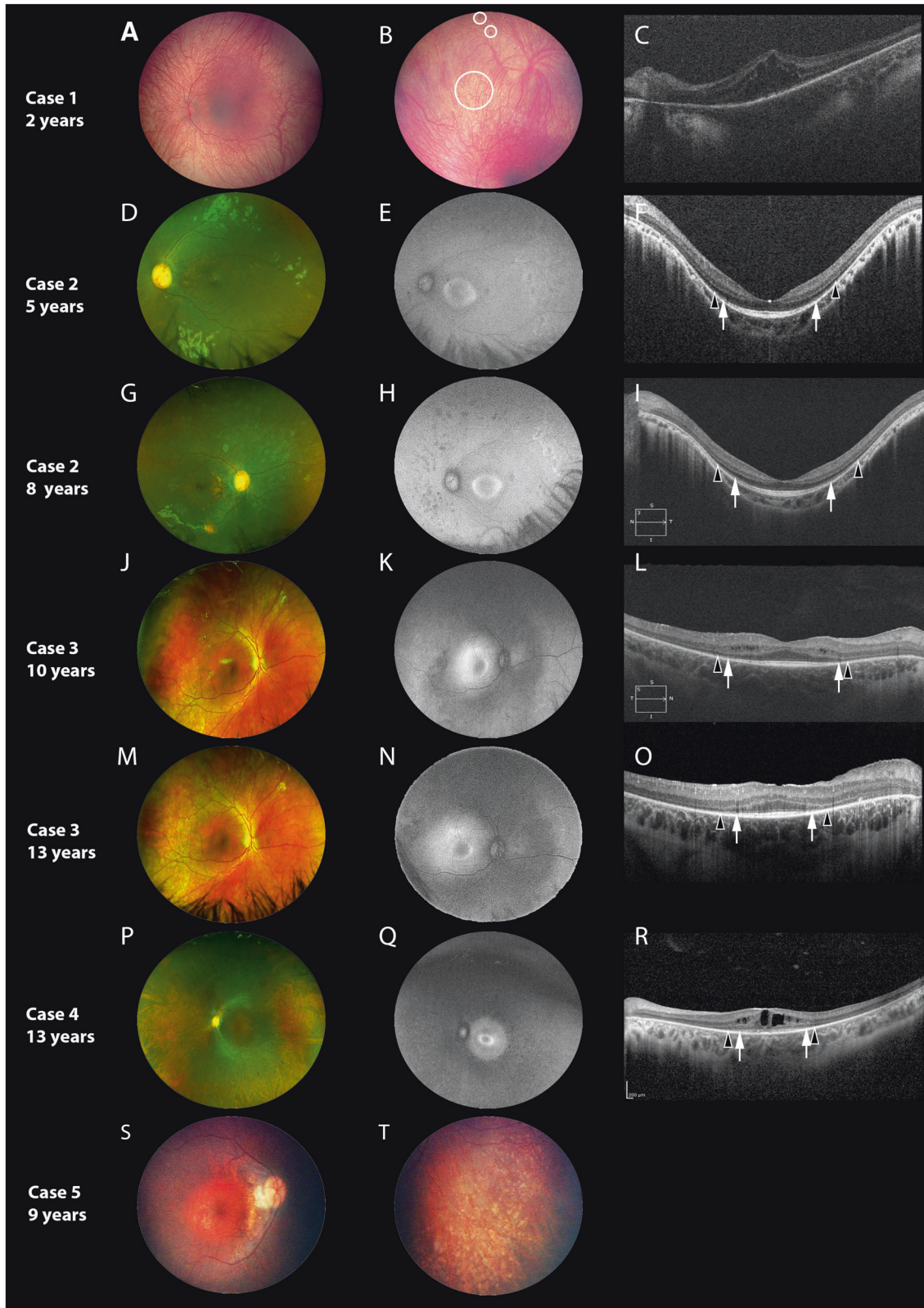
<sup>b</sup>Cases 9 and 10 are siblings.

<sup>c</sup>Previously reported: Merico et al. 2015.

<sup>d</sup>Previously reported: Dinur Schejter et al. 2017.

<sup>e</sup>Additional genetic findings: Microarray 6q24.1 deletion. Also, heterozygous stop variant in *GMAT1* (c.82 C > T, p.Arg28<sup>S</sup>); inherited from mother, but mother has normal eye exam, including ERG.





Three cases with distinct aspects are described individually.

**Case 1**

Case 1, an infant represents the youngest reported case of molecularly confirmed Roifman syndrome. At that young age,

the peripheral retina showed pigmentary changes and ERG showed severe generalized rod dysfunction and moderate to severe cone dysfunction (Supplementary Fig. 2A). There was marked foveo-macular retinoschisis with disruption of outer retinal lamination. At 2 years, parents observed the child to have

**Fig. 1 Retinal imaging of Cases 1–5.** Each horizontal panel represents a single patient visit with fundus photo, autofluorescence (FAF, if available) and optical coherence tomography (OCT, if available). **A–C** represent Case 1, **(D–I)** represent Case 2, **(J–O)** represent Case 3, **(P–R)** represent Case 4 and **(S, T)** represent Case 5. Cases are organized in terms of increasing age at characterization, with repeat imaging for Cases 2 and 3 provided at follow-up. *Black arrowheads* demarcate the preserved horizontal extent of the external limiting membrane (ELM); *white arrows* demarcate the extent of the ellipsoid zone (EZ). The fundus is characterized by retinal pigment epithelial and pigmentary changes along the arcades and mid-periphery, with associated arteriolar attenuation, without significant disc pallor. A dull foveal reflex is also characteristic. In the youngest patient (**A**) the fundus is blonde with prominent choroidal vasculature and no vessel attenuation, with pigmentary changes only visible in the far periphery (**B, circles**). A para-foveal (**Q**) or peri foveal (**E, H, K, N**) hyper autofluorescent ring was commonly observed. The ring demonstrated a reduction in diameter, becoming more distinct and closer to the foveal centre with increasing age. The peripheral areas of hypofluorescence on FAF corresponded well with the retinal areas of retinal atrophy. Findings on macular OCT are characterized by relatively preserved foveal outer nuclear layer, with most cases showing preservation of outer retinal lamination (EZ and ELM) in the central 2 mm (**F, I, L, O, R**). Around the margins of EZ loss, ELM could be identified. Three cases showed cystoid/schitic macular changes (**C, L, R**).

nyctalopia, whereas fundus showed distinct hyperpigmented spots in the mid-periphery (Fig. 1B) and persistent foveo-macular schisis (Fig. 1C).

### Case 5

Case 5 had the longest follow-up of 19 years (Figs. 1, 2). At first visit (6 years), the child was asymptomatic, but bilateral mild RPE changes and disc drusen were noted. At 9 years, nyctalopia was reported and fundus showed mid-peripheral pigmentary changes and bony spicules that progressed over time; progressive centripetal atrophy was noted over time. Mild cystoid changes were seen at 15 years of age that were not evident at 25 years (Fig. 2C and F). The EZ was mildly disrupted in the central 2 mm (15 years) that progressively shortened over time. Visual acuity in the right eye was similar at 15 and 25 years (20/100), whereas in the left, a single line deterioration was noted (20/70 to 20/80). The ERG was non-detectable at 19 years of age (Supplementary Fig. 2E; ERG was not performed at first visit).

### Case 6

Case 6 (Fig. 2 and supplemental Fig. 1), a 20-year-old female exhibited sectoral disease. She had no nyctalopia and demonstrated normal BCVA, color vision and contrast sensitivity. Fundus examination was characterized by inferior sectoral RPE disruption and pigmentary mottling more evident peripherally. FAF imaging showed a hyper-autofluorescent border surrounding the disc and encircling the inferior area of involvement. Macular autofluorescence was normal. Pattern ERG was normal and the full-field ERG showed isolated rod dystrophy. The SD-OCT scans from the affected areas showed loss of EZ, ELM and outer nuclear layer (Supplementary Fig. 1C–F). Macular scans were normal consistent with absence of macular involvement on funduscopy, FAF and pattern ERG.

### Genetic results

Genetic results are presented in Table 1. All subjects had biallelic disease causing variants in *RNU4ATAC*, including one in the stem II region (nucleotides 13–19). The second nucleotide alteration was in the 5' stem loop (7 cases), 3' stem loop (2 cases) or in the stem II region (Case 2). Case 5 had novel stem II (n.13 C > G) and 5' Stem-loop variants (n.29 T > C); other alterations at n.13 are known to cause Roifman syndrome [2] and n.30 G > A is known to cause MOPD1 [4].

### Systemic phenotype

Most patients suffered from hypogammaglobulinemia (Cases 2–7), agammaglobulinemia (Case 8), or dysgammaglobulinemia (Cases 1, 9, and 10). All patients exhibited characteristic developmental delay, a history of intrauterine growth restriction, and characteristic dysmorphism including skeletal or epiphyseal dysplasia (Table 1). Most had recurrent sinopulmonary infections (Cases 2–10) and otitis media (Cases 3, 5–7, 9, 10).

### DISCUSSION

This study provides the largest series and is the first comprehensive description of the ocular phenotype in *RNU4ATAC*-associated Roifman syndrome. The presence of a retinal dystrophy had been variably associated previously but not systematically characterized [1–3, 12]. In this series, all patients showed generalized retinal dysfunction on ERG, and all except one had rod-cone dystrophy on ERG. Overall, the retinal appearance was in keeping with retinitis pigmentosa (RP); notably, one individual had sectoral RP. However, unlike typical RP, *RNU4ATAC*-retinopathy was early in onset as all four cases examined in the first decade of life had abnormal retinal exam or ERG. There was evidence of slow disease progression on follow-up; this included loss of distance vision (2/6), ellipsoid zone width (1/6) and/or progressive mid-peripheral retinal changes (3/6). However, there was no significant relationship between age and BCVA decline for the entire cohort.

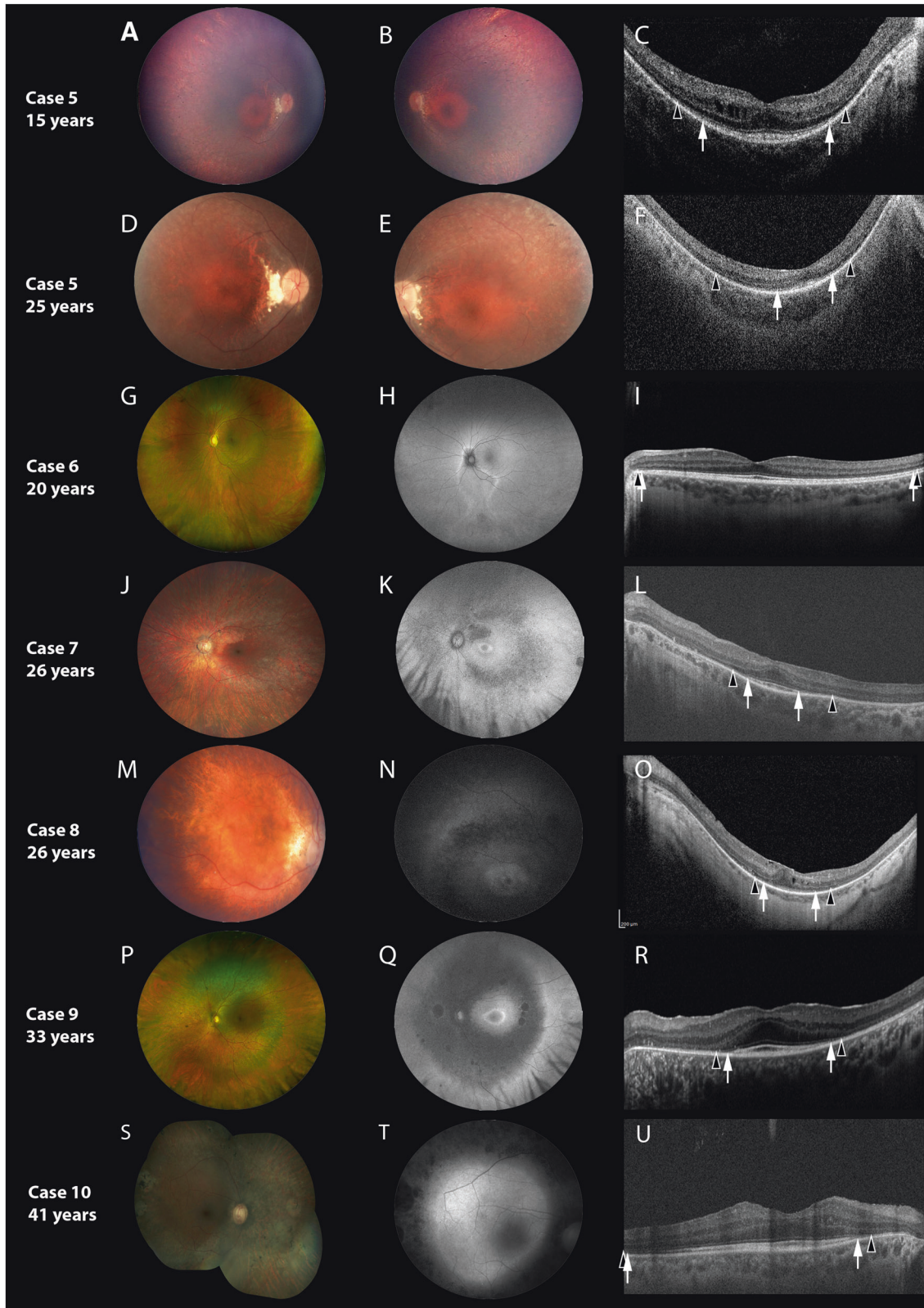
The majority of our patients (70%) had complaints of nyctalopia; age of onset was variable and likely relates to the disease severity. The youngest of these patients, a 2-year-old, had severe rod dystrophy on ERG. Interestingly, two patients who denied nyctalopia only had mild to moderate rod dystrophy on ERG (Cases 6 and 8). In literature, amongst cases of retinal dystrophy ( $n = 9$ ) [2, 3, 11, 12], nyctalopia was recorded only in 1 subject which happens to be Case 4 in the current study [3].

Central visual acuity was better than 20/50 (Age Range: 5–41 years) in at least one eye in 60% of our cases. Cases that had BCVA worse than 20/70 had notable disruption of sub-foveal EZ on OCT ( $n = 4$ ; age range 2–26 years). Two subjects showed  $\geq 2$ -line worsening in BCVA in at least one eye over time. Hence, the degree of visual loss is likely related to the outer retinal changes (on SD-OCT) and disease progression with age.

Most patients (9/10) exhibited generalized retinal changes similar to RP characterized by mid-peripheral atrophy, and pigmentary changes, akin to previously reported cases [2, 3, 11, 12]. In the infant patient in our cohort, pigmentary changes were visible in the far periphery, suggestive of early onset retinal involvement in Roifman syndrome. Further, in older patients, patches of scalloped RPE atrophy were observed in the mid-periphery, a novel observation. Our study is also unique for a case of macula sparing sectoral RP; upon careful review, a previous case in literature seems to have sectoral disease, although not specified by the authors [11].

On FAF imaging, a ring of abnormal hyper-autofluorescence at the macula suggesting aberrant lipofuscin accumulation was seen in majority (75%) of patients, and this is a novel observation in Roifman retinopathy. This hyper-autofluorescence ring, although non-specific, is commonly seen in RP [18] and is an indicator of disease-severity [19–21]. Similar parafoveal rings have been documented in other retinal dystrophies, including Leber congenital amaurosis [22], X-linked retinoschisis [23], and *RPGR* [24]-, *GUCA1A*- [25], *GUCY2D* [26]-associated cone-rod dystrophy. Further, the peripheral areas of hypo-autofluorescence found in our patients corresponded well with the areas of RPE atrophy on





fundus photos. Both patients who had serial FAF imaging (3 years apart) showed progressive increase in the areas of hypoautofluorescence suggesting disease progression. In our patient with sectoral retinal involvement (20-year-old), the involved regions were surrounded by a border of hyperautofluorescence;

our patient appeared to have a less severe phenotype than the 7-year-old previously documented with sectoral disease [11].

Subfoveal EZ and ELM was relatively preserved in 60% of cases, and these cases had better BCVA. The rest demonstrated disruption of central EZ and ELM, and hence had poorer visual

**Fig. 2 Detailed retinal characteristics of Cases 5–10.** Each horizontal panel represents a single patient visit with fundus photo, autofluorescence (FAF, if available) and optical coherence tomography (OCT). **A–F** Represent Case 5, **(G–I)** represent Case 6, **(J–L)** represent Case 7, **(M–O)** represent Case 8, **(P–R)** represent Case 9 and **(S–U)** represent Case 10. Cases are organized in terms of increasing age at characterization, with repeat imaging for Cases 5 provided at follow-up. *Black arrowheads* demarcate the preserved horizontal extent of the external limiting membrane (ELM); *white arrows* demarcate the extent of the ellipsoid zone (EZ). The fundus is characterized by retinal pigment epithelial and pigmentary changes along the arcades and mid-periphery, with associated arteriolar attenuation, without significant disc pallor. Bilateral disc drusen was observed in Case 5 (**D, E**). A parafoveal (**K, N**) or peri-foveal (**Q**) hyper autofluorescent ring was commonly observed. The peripheral areas of hypofluorescence corresponded well with the retinal areas of retinal atrophy. Cases 6 had normal macular autofluorescence (**H**) or whereas, Case 10 had generalized macular hyper autofluorescence, respectively (**T**). Widefield imaging in Case 6 shows (**G**) inferior sectoral RPE and pigmentary mottling; FAF (**H**) shows a corresponding area of sectoral hypo-autofluorescence, with a hyper-autofluorescent border. Two cases showed relative preservation of outer retinal lamination (EZ and ELM) across most of temporal macular line scan (**I, U**); whereas Case 5 at the last visit (**F**) and Case 8 (**O**) showed mild disruption of the sub-foveal EZ. Two cases showed mild cystoid macular changes (**C, O**).

acuity (worse than 20/70 in either eye). One subject (Case 5) with extended follow-up (10 years), showed progressive loss of parafoveal EZ and ELM. Posterior staphyloma was observed in 30% of cases; intriguingly, none of them were myopic.

The ERG results showed all subjects to have generalized rod dysfunction, and the rod system was equally or more severely affected than cone system in everyone suggesting a rod first involvement in *RNU4ATAC*-retinopathy. Further, all except case 6 had moderate to severe or very severe abnormality in the rod ERGs regardless of the age. Previous literature also showed severe rod and cone dysfunction [1] or isolated rod dysfunction (in the case with sectoral involvement) [11], similar to our results.

The majority of our patients (80%) had genotypes consisting of known variants involving the Stem II region [3] of *RNU4ATAC*, in *trans* with variants in non-Stem II regions that have been associated with Roifman syndrome [2]. Case 5 had a novel Stem II variant n.13 C > G; but other alterations involving the n.13 C nucleotide (n.13 C > T) have been reported in Roifman syndrome [2, 11]. Case 2 is one of only two patients ever reported with a homozygous Stem II variant (n.16 G > A) causing Roifman syndrome [3, 12]. Whilst Case-2 had severe generalized rod-cone dystrophy in childhood, the onset of retinal dystrophy was not described in the other subject [12]. Our case series had two female patients: one exhibiting early-onset pan-retinal disease (Case 2; n.16 G > A/n.16 G > A) and the other with a milder sectoral retinal disease as a young adult (Case 6; n.13 C > T/n.46 G > A). Of the female Roifman syndrome cases previously reported, Heremans et al. [12] described a case (n.16 G > A/n.46 G > A) with severe pan-retinal dystrophy (age of onset unknown), and Bogaert et al. [11] reported one (n.13 C > T/n.116 A > T) with mild retinal dystrophy (at 14 years). Taken together, this may perhaps suggest n.16 G > A and n.13 C > T alleles in females to be associated with severe and milder retinal phenotypes, respectively. A male harboring n.16 G > A allele (current study; Case 8) also demonstrated generalized retinal dystrophy. On the contrary, the n.13 C > T variant has been reported in males from different kinships with Roifman syndrome [2] and also seen in 4 males in our series in compound heterozygous state; all demonstrated generalized retinal dystrophy. In our study, three pairs of patients harbored the same variants in both alleles (Cases 1 and 4, Cases 3 and 7, and Cases 9 and 10); all demonstrated a generalized rod-cone dystrophy. No additional genotype phenotype correlation was noted.

*RNU4ATAC* homozygous or compound heterozygous variants limited to the 5' Stem-loop, Stem I, Sm protein binding site, and the 3' Stem-loop have been associated with MOPD1 [4, 5], a clinically distinct disorder [5]. Patients with MOPD1 lack the findings of epiphyseal dysplasia and immunodeficiency that are seen in Roifman syndrome. Further, MOPD1 is associated with retinal hypopigmentation without rod-cone degeneration [5, 27, 28]. Also, no patients with MOPD1 have ever been reported with a variant in the Stem II region. Hence, it is likely that the Stem II variant drives the retinal dystrophy phenotype in Roifman syndrome.

When reviewing prioritized genes with splicing alterations identified in Roifman syndrome [2], and which have been reported

to have phenotypes that might be relevant to Roifman syndrome and retinopathies, the most compelling candidates were *XRCC5*, *ALG12* and *HTT*. Mouse knockout models of *Xrcc5*<sup>-/-</sup> exhibit growth retardation, severe combined immunodeficiency and retinal abnormalities [29–31]. *HTT* encodes the Huntingtin protein, and mice models show retinal degeneration; [32, 33] but Huntington disease shows an insufficient phenotypic match to Roifman syndrome. *ALG12* is an alpha-1,6-mannosyltransferase implicated in recessive glycosylation disorder [34], and has a systemic phenotypic presentation akin Roifman syndrome. But retinal degeneration has never been reported in *ALG12*-related disorder [35, 36]. Hence, the pathogenesis of retinal involvement in Roifman syndrome is still unknown.

In summary, we have detailed and refined the ocular phenotypic characteristics of *RNU4ATAC*-associated Roifman syndrome spanning four decades. The retinopathy is universal, early-onset, and shows slow progression. The disease generally shows a rod-cone dystrophy pattern and has similarities to RP. We also highlight sectoral RP at the mild end of the spectrum of Roifman retinopathy. In younger affected, the OCT demonstrates reasonable preservation of sub-foveal photoreceptors, and hence, distance vision is relatively preserved at presentation. Half of the patients demonstrated cystoid/schitic macular changes at some stage of the disease. This study highlights the need for detailed ocular phenotyping in Roifman syndrome patients to characterize disease onset and progression. Our results and literature review surrounding the various phenotypes reported with *RNU4ATAC* suggests an allelic hierarchy of Stem II variants to cause retinal dystrophy. In future, larger cohorts will help to better understand how disease-causing variants might interact in an allelic hierarchy and help ascertain if there are sex-related differences in disease severity.

Supplemental information is available at Eye's website.

## SUMMARY

What was known before

- Roifman syndrome is an autosomal recessive disorder due to disease causing variants in *RNU4ATAC*.
- Immunodeficiency, spondyloepiphyseal dysplasia, developmental delay and facial dysmorphism are common manifestations.
- Retinal involvement is variable, reported in half of the reported cases. The retinal phenotype is not well characterized.

What this study adds

- Roifman syndrome is associated with a slow, progressive, early-onset retinal dystrophy that affects all patients.

- The retinal phenotype commonly manifests as a generalized rod-cone dystrophy, and fundus, autofluorescence and optical coherence tomography show similarities to retinitis pigmentosa.
- Sectoral retinal involvement is a rare ocular manifestation of Roifman syndrome

## DATA AVAILABILITY

All data generated or analyzed during this study are included in this published paper. Further queries can be directed to the corresponding author.

## REFERENCES

1. Roifman CM. Antibody deficiency, growth retardation, spondyloepiphyseal dysplasia and retinal dystrophy: a novel syndrome. *Clin Genet.* 1999;55:103–9.
2. Merico D, Roifman M, Braunschweig U, Yuen RK, Alexandrova R, Bates A, et al. Compound heterozygous mutations in the noncoding RNU4ATAC cause Roifman Syndrome by disrupting minor intron splicing. *Nat Commun.* 2015;6:8718.
3. Dinur Schejter Y, Ovadia A, Alexandrova R, Thiruvahindrapuram B, Pereira SL, Manson DE, et al. A homozygous mutation in the stem II domain of RNU4ATAC causes typical Roifman syndrome. *NPJ Genom Med.* 2017;2:23.
4. He H, Liyanarachchi S, Akagi K, Nagy R, Li J, Dietrich RC, et al. Mutations in U4atac snRNA, a component of the minor spliceosome, in the developmental disorder MOPD I. *Science* 2011;332:238–40.
5. Abdel-Salam GM, Miyake N, Eid MM, Abdel-Hamid MS, Hassan NA, Eid OM, et al. A homozygous mutation in RNU4ATAC as a cause of microcephalic osteodysplastic primordial dwarfism type I (MOPD I) with associated pigmentary disorder. *Am J Med Genet A.* 2011;155A:2885–96.
6. Robertson SP, Rodda C, Bankier A. Hypogonadotrophic hypogonadism in Roifman syndrome. *Clin Genet.* 2000;57:435–8.
7. Mandel K, Grunebaum E, Benson L. Noncompaction of the myocardium associated with Roifman syndrome. *Cardiol Young.* 2001;11:240–3.
8. de Vries PJ, McCartney DL, McCartney E, Woolf D, Wozencroft D. The cognitive and behavioural phenotype of Roifman syndrome. *J Intellect Disabil Res.* 2006;50:690–6.
9. Gray PE, Sillence D, Kakakios A. Is Roifman syndrome an X-linked ciliopathy with humoral immunodeficiency? Evidence from 2 new cases. *Int J Immunogenet.* 2011;38:501–5.
10. Fairchild HR, Fairchild G, Tierney KM, McCartney DL, Cross JJ, de Vries PJ. Partial agenesis of the corpus callosum, hippocampal atrophy, and stable intellectual disability associated with Roifman syndrome. *Am J Med Genet A.* 2011;155A:2560–5.
11. Bogaert DJ, Dullaers M, Kuehn HS, Leroy BP, Niemela JE, De Wilde H, et al. Early-onset primary antibody deficiency resembling common variable immunodeficiency challenges the diagnosis of Wiedeman-Steiner and Roifman syndromes. *Sci Rep.* 2017;7:3702.
12. Heremans J, Garcia-Perez JE, Turro E, Schlenner SM, Casteels I, Collin R, et al. Abnormal differentiation of B cells and megakaryocytes in patients with Roifman syndrome. *J Allergy Clin Immunol.* 2018;142:630–46.
13. Hallermayr A, Graf J, Koehler U, Laner A, Schonfeld B, Benet-Pages A, et al. Extending the critical regions for mutations in the non-coding gene RNU4ATAC in another patient with Roifman Syndrome. *Clin Case Rep.* 2018;6:2224–8.
14. Clifford D, Moloney F, Leahy TR, Murray DM. Roifman syndrome: a description of further immunological and radiological features. *BMJ Case Rep.* 2022;15:e249109.
15. Chandrakumar M, Colpa L, Reginald YA, Goltz HC, Wong AM. Measuring contrast sensitivity using the M&S Smart System II versus the Pelli-Robson chart. *Ophthalmology* 2013;120:2160–1.
16. Robson AG, Frishman LJ, Grigg J, Hamilton R, Jeffrey BG, Kondo M, et al. ISCEV Standard for full-field clinical electroretinography (2022 update). *Doc Ophthalmol.* 2022;144:165–77.
17. Bach M, Brigell MG, Hawlina M, Holder GE, Johnson MA, McCulloch DL, et al. ISCEV standard for clinical pattern electroretinography (PERG): 2012 update. *Doc Ophthalmol.* 2013;126:1–7.
18. Robson AG, Egan C, Holder GE, Bird AC, Fitzke FW. Comparing rod and cone function with fundus autofluorescence images in retinitis pigmentosa. *Adv Exp Med Biol.* 2003;533:41–7.
19. Robson AG, Michaelides M, Saihan Z, Bird AC, Webster AR, Moore AT, et al. Functional characteristics of patients with retinal dystrophy that manifest abnormal parafoveal annuli of high density fundus autofluorescence; a review and update. *Doc Ophthalmol.* 2008;116:79–89.
20. Robson AG, Saihan Z, Jenkins SA, Fitzke FW, Bird AC, Webster AR, et al. Functional characterisation and serial imaging of abnormal fundus autofluorescence in patients with retinitis pigmentosa and normal visual acuity. *Br J Ophthalmol.* 2006;90:472–9.
21. Robson AG, El-Amir A, Bailey C, Egan CA, Fitzke FW, Webster AR, et al. Pattern ERG correlates of abnormal fundus autofluorescence in patients with retinitis pigmentosa and normal visual acuity. *Investig Ophthalmol Vis Sci.* 2003;44:3544–50.
22. Scholl HP, Chong NH, Robson AG, Holder GE, Moore AT, Bird AC. Fundus autofluorescence in patients with leber congenital amaurosis. *Investig Ophthalmol Vis Sci.* 2004;45:2747–52.
23. Tsang SH, Vaclavik V, Bird AC, Robson AG, Holder GE. Novel phenotypic and genotypic findings in X-linked retinoschisis. *Arch Ophthalmol.* 2007;125:259–67.
24. Robson AG, Michaelides M, Luong VA, Holder GE, Bird AC, Webster AR, et al. Functional correlates of fundus autofluorescence abnormalities in patients with RPGR or RIMS1 mutations causing cone or cone rod dystrophy. *Br J Ophthalmol.* 2008;92:95–102.
25. Michaelides M, Wilkie SE, Jenkins S, Holder GE, Hunt DM, Moore AT, et al. Mutation in the gene GUCA1A, encoding guanylate cyclase-activating protein 1, causes cone, cone-rod, and macular dystrophy. *Ophthalmology* 2005;112:1442–7.
26. Downes SM, Payne AM, Kelsell RE, Fitzke FW, Holder GE, Hunt DM, et al. Autosomal dominant cone-rod dystrophy with mutations in the guanylate cyclase 2D gene encoding retinal guanylate cyclase-1. *Arch Ophthalmol.* 2001;119:1667–73.
27. Abdel-Salam GM, Abdel-Hamid MS, Hassan NA, Issa MY, Effat L, Ismail S, et al. Further delineation of the clinical spectrum in RNU4ATAC related microcephalic osteodysplastic primordial dwarfism type I. *Am J Med Genet A.* 2013;161A:1875–81.
28. Abdel-Salam GM, Abdel-Hamid MS, Issa M, Magdy A, El-Kotoury A, Amr K. Expanding the phenotypic and mutational spectrum in microcephalic osteodysplastic primordial dwarfism type I. *Am J Med Genet A.* 2012;158A:1455–61.
29. Nussenzweig A, Chen C, da Costa Soares V, Sanchez M, Sokol K, Nussenzweig MC, et al. Requirement for Ku80 in growth and immunoglobulin V(D)J recombination. *Nature* 1996;382:551–5.
30. Karanjawala ZE, Hinton DR, Oh E, Hsieh CL, Lieber MR. Developmental retinal apoptosis in Ku86<sup>-/-</sup> mice. *DNA Repair (Amst).* 2003;2:1429–34.
31. Zhu C, Bogue MA, Lim DS, Hasty P, Roth DB. Ku86-deficient mice exhibit severe combined immunodeficiency and defective processing of V(D)J recombination intermediates. *Cell* 1996;86:379–89.
32. Helmlinger D, Yvert G, Picaud S, Merienne K, Sahel J, Mandel JL, et al. Progressive retinal degeneration and dysfunction in R6 Huntington's disease mice. *Hum Mol Genet.* 2002;11:3351–9.
33. Karam A, Tebbe L, Weber C, Messaddeq N, Morle L, Kessler P, et al. A novel function of Huntingtin in the cilium and retinal ciliopathy in Huntington's disease mice. *Neurobiol Dis.* 2015;80:15–28.
34. Chantret I, Dupre T, Delenda C, Bucher S, Dancourt J, Barnier A, et al. Congenital disorders of glycosylation type Ig is defined by a deficiency in dolichyl-P-mannose:Man7GlcNAc2-PP-dolichyl mannosyltransferase. *J Biol Chem.* 2002;277:25815–22.
35. Zdebska E, Bader-Meunier B, Schischmanoff PO, Dupre T, Seta N, Tchernia G, et al. Abnormal glycosylation of red cell membrane band 3 in the congenital disorder of glycosylation Ig. *Pediatr Res.* 2003;54:224–9.
36. Kranz C, Basinger AA, Guccasavas-Calikoglu M, Sun L, Powell CM, Henderson FW, et al. Expanding spectrum of congenital disorder of glycosylation Ig (CDG-Ig): sibs with a unique skeletal dysplasia, hypogammaglobulinemia, cardiomyopathy, genital malformations, and early lethality. *Am J Med Genet A.* 2007;143A:1371–8.

## ACKNOWLEDGEMENTS

We thank the patients for their active participation in the study. We thank Leslie MacKeen and Cynthia VandenHoven, for their assistance with obtaining multi-modal imaging. EH is supported by the Henry Brent Chair in Innovative Pediatric Ophthalmology Research.

## AUTHOR CONTRIBUTIONS

CMR and AV designed the study concept. BGB, AM, AT (ATumber), JG, EH, CMR and AV collected data. BGB, AM, AT (ATumber) and AV analyzed the data. BGB, AM, AT (ATayyib), AT (ATumber), LV, CMR and AV wrote the first draft of the paper. All authors contributed to the final draft of the paper and approved the contents.

## FUNDING

AV is supported by the Foundation Fighting Blindness, USA (CD-CL-0617-0727-HSC).

## COMPETING INTERESTS

The authors declare no competing interests.



### ADDITIONAL INFORMATION

**Supplementary information** The online version contains supplementary material available at <https://doi.org/10.1038/s41433-023-02581-1>.

**Correspondence** and requests for materials should be addressed to Ajoy Vincent.

**Reprints and permission information** is available at <http://www.nature.com/reprints>

**Publisher's note** Springer Nature remains neutral with regard to jurisdictional claims in published maps and institutional affiliations.